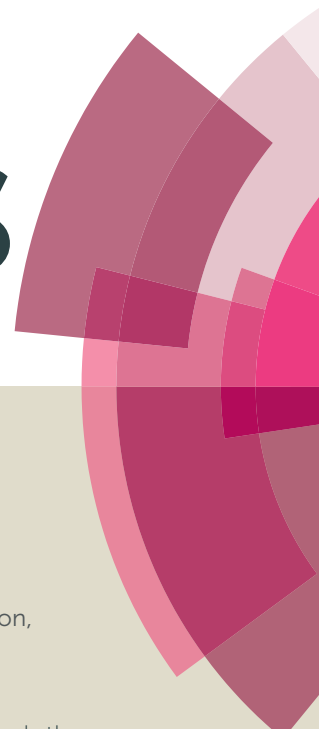


RSC Advances



This article can be cited before page numbers have been issued, to do this please use: K. Lee, J. W. Jeon, B. M. Maeng, K. M. Huh, J. C. Won, Y. Yoo, Y. S. Kim and B. G. Kim, *RSC Adv.*, 2016, DOI: 10.1039/C6RA13034H.



This is an *Accepted Manuscript*, which has been through the Royal Society of Chemistry peer review process and has been accepted for publication.

Accepted Manuscripts are published online shortly after acceptance, before technical editing, formatting and proof reading. Using this free service, authors can make their results available to the community, in citable form, before we publish the edited article. This *Accepted Manuscript* will be replaced by the edited, formatted and paginated article as soon as this is available.

You can find more information about *Accepted Manuscripts* in the [Information for Authors](#).

Please note that technical editing may introduce minor changes to the text and/or graphics, which may alter content. The journal's standard [Terms & Conditions](#) and the [Ethical guidelines](#) still apply. In no event shall the Royal Society of Chemistry be held responsible for any errors or omissions in this *Accepted Manuscript* or any consequences arising from the use of any information it contains.



RSC Advances

PAPER

Synthesis and Characterization of Polyethersulfone with Intrinsic Microporosity

Kyuchul Lee,^{ab} Jun Woo Jeon,^{ab} Bo Mi Maeng,^{ac} Kang Moo Huh,^c Jong Chan Won,^{ab} Youngjae Yoo,^{ab} Yong Seok Kim,^{*ab} Byoung Gak Kim^{*ab}

Received 00th January 20xx,
Accepted 00th January 20xx

DOI: 10.1039/x0xx00000x

www.rsc.org/

Polymers of intrinsic microporosity (PIMs¹) are usually ladder-type polymers that adopt a spiro structure. In the present study, a new non-ladder-type polyethersulfone-type PIM that incorporated a linear sulfone moiety was synthesized. Brunauer–Emmett–Teller measurements confirmed that the synthesized polymer had a high specific surface area (430–590 m² g⁻¹) due to the presence of micropores of size 0.54–0.66 nm. Intrinsic porosity characteristics of the new PIM are attributed to the resonance structures of sulfone and benzene moieties. Syntheses of new gas-separation membrane using PIMs containing sulfone or similar functional groups are expected in the future.

Introduction

All polymers possess fine pores or free volume. However, most noncrystalline polymers comprise highly mobile polymer chains such that the polymer chains are effectively tightly packed; the resultant compact polymers are generally classified as nonporous materials. However, there is an exception as well: noncrystalline polymers of intrinsic microporosity (PIMs) that are very rigid, and their twisted molecular structure prevents polymer chain alignment.¹ They have fine pores of ≤ 2 nm and show very high specific surface area of 500–1000 m² g⁻¹.^{2–7}

Several PIMs adopt spiro structures, i.e., they have twisted molecular structures. When polymers chains take spiro structures, interactions between the polymer chains reduce, thus increasing the polymer's free volume and giving rise to microporosity. Consequently, such polymers have a large specific surface area. Moreover, spiro structures undergo ladder-type linking that further hinders the free rotation of polymer chains. Some prime examples of such polymers are PIM-1 and PIM-7. Introduction of dinaphthyl, hexaphenylbenzene, and triptycene structures, rather than spiro structure, have been reported for application in gas-separation membranes.^{8–11} Modification of PIMs such as carboxylated PIM, triazine-PIM, sulfonation-PIM, PIM–CF₃, PIM-tetrazole, PIM-amine, PIM-azide, PIM-thioamide, and PIM-amidoxime have also been reported.^{11–19} PIMs find

applications in other fields also, including ionic diodes and rectifiers, as well as organic photovoltaic electrodes owing to the carbonization of the PIM-1 polymer.^{20–22} However, very few studies have investigated new monomers that can be used the connection area of PIM, creating hurdles in polymer design.

One possible candidate for the non-ladder type connection is the sulfonyl group. For example, polyethersulfone that have sulfonyl (–SO₂–), ether (–O–), and isopropylidene (–C(CH₃)₂–) groups linked to a benzene ring, whose advantageous features such as high thermal properties and strong mechanical properties are due to the strong resonance of sulfonyl group within the polyethersulfone polymer chain.^{23–27}

Consequently, the degree of freedom in the polymer chain reduces that helps fabricate highly rigid polymer chains with relatively strong mechanical properties and high heat resistance. The resonance structures of the sulfonyl group have different thermal stabilities and polymer chain strengths, depending on the position of the sulfonyl group on the benzene ring. The sulfonyl group in the para (*p*) position has two resonance structures, whereas in the meta (*m*) position, it has only one resonance structure. Thus, higher heat resistance and stronger mechanical properties are observed for structures with *p*-sulfonyl groups on the benzene rings.²⁸

Accordingly, we aimed to synthesize polyethersulfone with excellent thermal stability and microporosity by introducing a linear sulfonyl group, abandoning the ladder-type framework that is the main characteristic of PIMs, and to examine the characteristics of such polyethersulfones.

Experimental

Chemical reagents

^a Advanced Material Division, Korea Research Institute of Chemical Technology, 141 Gajeong-ro, Yuseong-gu, Daejeon, 34114, Republic of Korea, E-mail: yongskim@kRICT.re.kr (Y. S. Kim), bkim@kRICT.re.kr (B. G. Kim).

^b Department of Nanomaterials Science and Engineering and Department of Chemical Convergence Materials, University of Science & Technology, 217 Gajeong-ro, Yuseong-gu, Daejeon, 34113, Republic of Korea.

^c Department of Polymers Science and Engineering, Chungnam National University, 99 Daehak-ro, Yuseong-gu, Daejeon, 34134, Republic of Korea.

1,2-Difluorobenzene, aluminum chloride (TCl), chlorosulfonic acid, potassium carbonate (99.99%, Sigma-Aldrich), and magnesium sulfate (Sigma-Aldrich) were used as received. 5, 5'-6,6'-Tetrahydroxy-3,3,3'-tetramethyl-1,1'-spirobisindane (TTSBI, >97%, TCI) was purified by recrystallization from dichloromethane-methanol. Tetrafluoroterephthalonitrile (TFTPN, >98% Matrix Scientific) was purified by vacuum sublimation at 150 °C under an inert atmosphere. Toluene, dimethylformamide (DMF), methanol, and ethanol were used as received from standard vendors.

Synthesis of the monomers

Synthesis of 3,3',4,4'-teterfluorodiphenylsulfone (TFDPS) was similar to that reported by Wang et al.²⁹ 1,2-Difluorobenzene (10.3 g, 90 mmol) was gradually added into chlorosulfonic acid (33.7 g, 250 mmol) in a 100 mL 2-neck round flask at 0 °C. The resulting solution was stirred at 80 °C for 1 h and was then poured into ice-cold water. The product was extracted with dichloromethane. The organic extracts were washed with distilled water, dried over magnesium sulfate, and filtered, and the solvent was removed at 60 °C by vacuum drying. 3,4-Difluorobenzene-1-sulfonyl chloride (18.0 g, 94 %) was obtained as a pale yellow liquid.

3,4-Difluorobenzene-1-sulfonyl chloride (5.3 g, 25 mmol) and 1,2-difluorobenzene (11.4 g, 100 mmol) were added into a 100 mL round flask under nitrogen flow. Then, about 1 equiv of AlCl₃ (5.3 g, 25 mmol) was added into the mixture at 80 °C. Gaseous hydrogen chloride is evolved and is vented out through the teflon tubing. After emission of hydrogen chloride, the solution was heated to 100 °C and stirred for 8 h at 100 °C. The solution was cooled to room temperature and poured into crushed ice with stirring. The precipitate was obtained by vacuum filtration and washed with distilled water until a neutral filtrate was obtained. The dried crude product was recrystallized from ethanol twice and vacuum dried at 60 °C 24 h. TFDPS was obtained in 75% yield. The reaction scheme is shown in Fig 1.

Synthesis of PIM-1

TTSBI (3.40 g, 10 mmol), anhydrous K₂CO₃ (4.14 g, 30 mmol), TFTPN (2.00 g, 10 mmol), and DMF (70 mL) were added to a 250-mL 2-necked flask fitted with a condenser under a nitrogen gas flow. The reaction mixture was stirred at 55 °C for 72 h. The resulting viscous solution was poured into water and the crude product collected by filtration. It was then dissolved in THF and reprecipitated from methanol twice. A 75% yield of yellow polymer (PIM-1) was obtained after complete vacuum drying; $M_n = 36,000$, PDI = 2.7 by gel permeation chromatography (GPC), calculated against polystyrene standards.

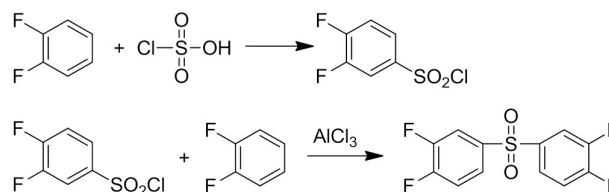


Fig 1. Synthesis scheme of TFDPS.

Synthesis of polyethersulfone with intrinsic microporosity (PESIM)

PESIM was synthesized as shown in Fig 2 (a). TTSBI (3.40 g, 10 mmol), anhydrous K₂CO₃ (4.14 g, 30 mmol), DMF (30 mL), and toluene (10 mL) were added to a 100-mL 2-necked flask fitted with a Dean-Stark trap and a condenser under a nitrogen gas flow. The reaction mixture was immersed in an oil bath maintained at 140 °C 1 h for remove water. Then, TFDPS (2.90 g, 10 mmol) was added to the flask, and the reaction mixture was heated 160 °C and then refluxed for 90 min under a nitrogen gas flow. The viscous solution was poured into water at room temperature and the crude product was collected by filtration. It was then dissolved in THF and reprecipitated from methanol twice. A pale brown polymer (PESIM) was obtained in 76% yield after complete vacuum drying; $M_n = 24,500$, PDI = 3.0 by GPC, calculated against polystyrene standards (Fig 3).

Synthesis of copolymers PESIM-75 and PESIM-25

PESIM-75 (75 monomer units) and PESIM-25 (25 monomer units) were synthesized as shown in Fig 2(b). TTSBI (3.40 g, 10 mmol), anhydrous K₂CO₃ (4.14 g, 30 mmol), DMF (30 mL), and toluene (10 mL) were added to a 100-mL 2-necked flask fitted with a Dean-Stark trap and a condenser under a nitrogen gas flow. The reaction mixture was immersed in an oil bath maintained 140 °C for 1 h to remove water. Then, TFTPN and TFDPS:TFDPS = 1:3 for PESIM-75 and TFTPN:TFDPS = 3:1 for PESIM-25 were added to the flask, and the reaction mixture was heated to 160 °C and refluxed for 90 min under a nitrogen gas flow. The viscous solution was poured into water and the crude product was collected by filtration. It was then dissolved in THF and reprecipitated from methanol twice. Yellow copolymers PESIM-75 and PESIM-25 were obtained in 75% yield after complete vacuum drying; $M_n = 14,000$, PDI = 3.0 (PESIM-75), $M_n = 16,000$, PDI = 3.1 (PESIM-25) by GPC, calculated against polystyrene standards.

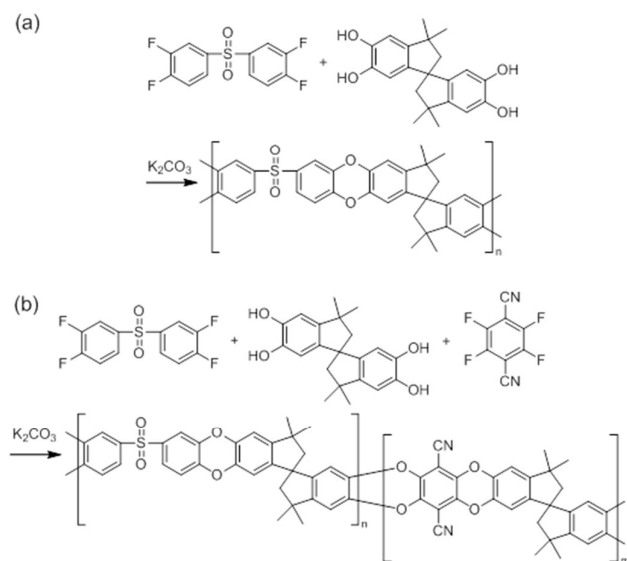


Fig 2. (a) Synthesis scheme of PESIM, (b) synthesis scheme of copolymers.

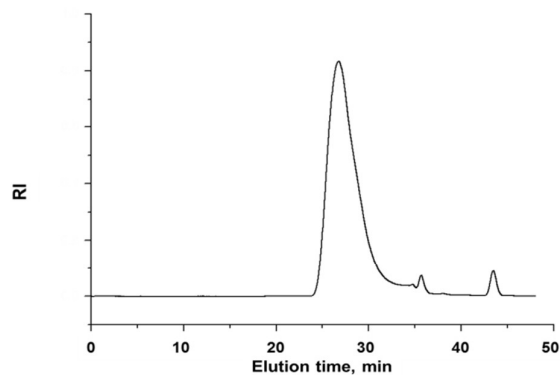


Fig 3. GPC curve of the polyethersulfone with intrinsic microporosity (PESIM).

Thermogravimetric analyses (TGA)

To determine their thermal stability, a thermogravimetric analyzer was used to identify the thermal decomposition behavior of PESIM, PESIM-75, PESIM-25 and PIM-1. PESIM and the copolymers were sufficiently dried before measuring their thermal decomposition behavior. TGA was taken from 30 °C to 600 °C at a heating rate of 10 °C/min in a nitrogen atmosphere using TA Instruments TGA Q500 at a heating rate of 10 °C/min.

Measurement of specific surface area

Microporous structures and specific surface areas of PESIM, PESIM-75, PESIM-25, and PIM-1 were determined via Brunauer–Emmett–Teller (BET) analysis. BET analysis was performed with Micromeritics ASAP 2420. Nitrogen was used as the adsorption/desorption gas and the analysis was performed by completely removing the moisture through a pre-treatment process at 200 °C.

Characterization methods

The structures of the synthesized monomer and PESIM-copolymers were fully characterized using both $^1\text{H-NMR}$ and $^{19}\text{F-NMR}$ spectroscopy. The NMR spectra were measured in CDCl_3 , DMSO-d_6 with a Bruker Advance 700 MHz spectrometer. The molecular weight and molecular weight distributions of the homo and copolymers were measured by GPC using Shodex columns (KF-800 series) and THF as the eluent at a flow rate of 1 mL/min. Signals were detected with a refractive index (RI) (Wyatt WREX-06) detector. The values obtained were determined by comparing them with a series of polystyrene standards. Glass-transition temperatures (T_g) were observed from differential scanning calorimetry (DSC) (Perkin-Elmer Diamond DSC), and samples for DSC were heated at 10 °C/min under a nitrogen flow and then quenched and reheated to measure the T_g values.

Results and Discussion

TFDPS structure analysis

The structure of TFDPS was identified by $^1\text{H-NMR}$ spectroscopy (Fig 4).

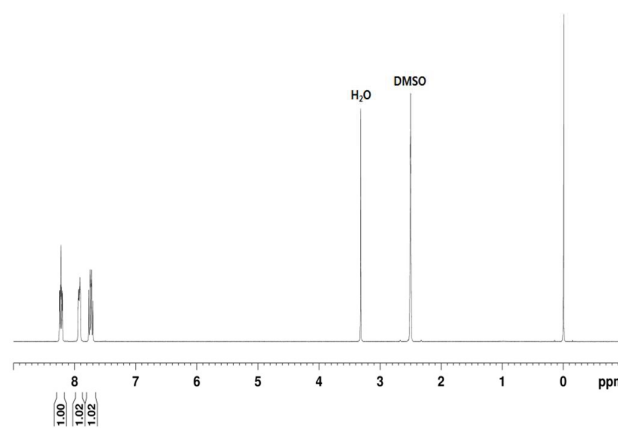


Fig 4. NMR spectrum of TFDPS.

PESIM, PESIM-75, and PESIM-25 structure analysis

The structures of PESIM, PESIM-75, and PESIM-25 were confirmed via $^1\text{H-NMR}$. The $^1\text{H-NMR}$ spectrum of PESIM is depicted in Fig 5. The integral ratio of PESIM's aromatic hydrogens c, d, e, and f to the spiro structure's hydrogens a and b was 6:2:1:1:1:1, which corresponds to the theoretical value. The integral ratios of the aromatic hydrogens of polyethersulfone in PESIM-75 and PESIM-25 to those of PIM-1 were 3:1 and 1:3, respectively. No peaks were seen in the $^{19}\text{F-NMR}$ spectrum of PIM; thus, it can be inferred that the TFDPS monomer was entirely consumed in the polymerization step.

hydrogens of polyethersulfone in PESIM-75, and PESIM-25.

Table 1. Thermal properties and Microporosity results of PESIM, PESIM-75, 25 and PIM-1

Sample	$T_{d5\%}$ ($^{\circ}\text{C}$)	$T_{d10\%}$ ($^{\circ}\text{C}$)	Surface area ($\text{m}^2 \cdot \text{g}^{-1}$)	Micropore size (nm)	Micropore volume ($\text{cm}^3 \cdot \text{g}^{-1}$)	Average pore diameter (nm)
PESIM	417	452	428	0.56	0.15	7.19
PESIM-75	463	484	480	0.66	0.19	7.11
PESIM-25	483	508	590	0.54	0.27	6.57
PIM-1	499	513	689	0.59	0.35	3.75

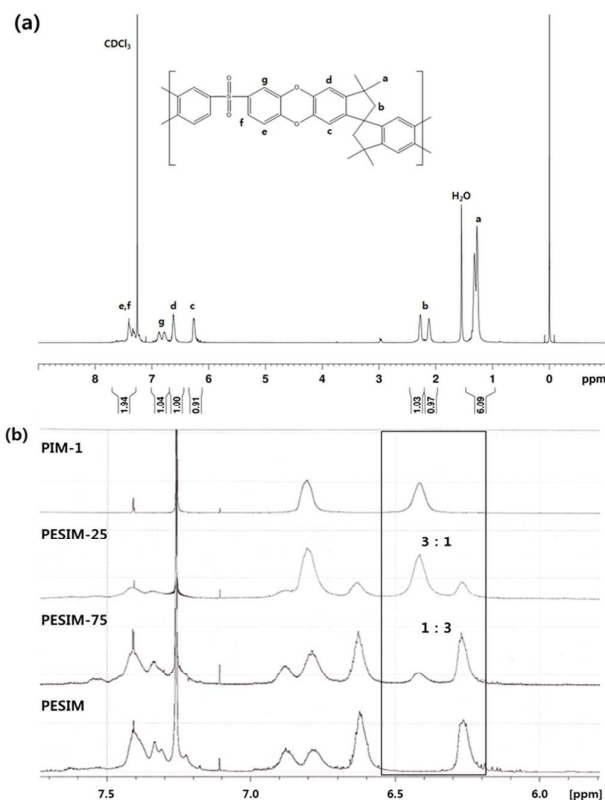


Fig 5. (a) NMR spectrum of PESIM, and (b) integral ratios of the aromatic

Thermal property analysis

The TGA results are shown in Table 1. Polyethersulfone is very rigid and has high thermal stability, because the degree of freedom in the polyethersulfone chain is suppressed by the strong resonance of the sulfonyl group. PESIM was also expected to have a very rigid polymer chain due to its twisted spiro structure and the strong resonance of the sulfonyl group. TGA curve of PESIM is shown in Fig 6. For PESIM, TGA results in 5% and 10% weight reduction at 417 $^{\circ}\text{C}$ and 452 $^{\circ}\text{C}$, respectively. For PESIM-75 and PESIM-25, high thermal stabilities of ≥ 400 $^{\circ}\text{C}$ were obtained, despite the fact that an increase in the amounts of monomers decreases the thermal stability relative to that of PIM-1. Noncrystalline polymers such as polyethersulfones have a T_g which is easy to detect, unlike crystalline polymers. T_g is affected by the size of the

substituents within the polymer chain and by their polarity, hydrogen bonding, and presence of aromatic rings. In the case of polyethersulfone, although structural variations lead to variations in T_g , it typically has a T_g of 225 $^{\circ}\text{C}$. Although PIM is a ladder-type noncrystalline polymer, its T_g cannot be identified below its decomposition temperature because T_g of PIM-1 is higher than decomposition temperature of PIM-1.² In order to identify the T_g of the synthesized polymer, measurements were taken over 50–350 $^{\circ}\text{C}$ at a speed of 10 $^{\circ}\text{C}/\text{min}$, but T_g could not be identified because multiple aromatic rings with outstanding symmetry had been introduced on the polymer chain of polyethersulfone with PIM, thus increasing the T_g value. Moreover, the polymer chain became rigid because of the resonance shown by the sulfonyl group. The T_g of PESIM-75 and PESIM-25 also could not be determined over 50–350 $^{\circ}\text{C}$.

BET analysis

The results of the BET analysis are shown in Table 1. The synthesized polymer with a wide specific surface area was confirmed through the adsorption and desorption isotherms, t-plot, and Horvath-Kawazoe (H-K) plot obtained from the analysis. The adsorption/desorption isothermal curve of PESIM is shown in Fig. 7 (a); a BET specific surface area of $428 \text{ m}^2 \cdot \text{g}^{-1}$ was obtained. A large amount of nitrogen adsorption occurred at a relatively low pressure range of the adsorption/desorption isothermal curve. This is a typical phenomenon of substances with micropores; hence, large adsorption at low pressures implies that the synthesized polymer has micropores. Moreover, the adsorption isothermal curve did not match the desorption isothermal curve; it showed a slight gap because desorption of nitrogen in micropores is slower than the rate of desorption of all nitrogen adsorbed at the same pressure.

In order to determine the sizes and volumes of the micropores, the t-plot, and H-K plot of the synthesized polymer were analyzed (Fig. 7 (b) and (c), respectively). The pressures at which the t-plot shows significant changes in the slope are related to the pore size: a change in the slope at a low pressure indicates decrease in the pore size. Since the slope changed at a low pressure in the t-plot, it was concluded that the synthesized polymer had micropores. Using the H-K plot shown in Fig 7 (c), the mean size and volume of the pores were confirmed to be 0.56 nm and $0.15 \text{ cm}^3 \cdot \text{g}^{-1}$, respectively.

A large amount of nitrogen adsorption at relatively low pressures also occurred in copolymers PESIM-75 and PESIM-25. Increase in the amount of sulfone-containing monomers lowered the specific surface area, pore size, and pore volume of the copolymers compared to those of PIM-1. The size of the micropores ranged from 0.54 to 0.66 nm for all polymers, but appreciable differences were observed in the mean diameter of the pores. Although the degree of freedom in the polymer chain is suppressed by the resonance of the sulfonyl group, the mean pore diameter is greater because the degree of freedom in the sulfone containing polymer chain is still higher than the polymer chain of PIM-1. Thus, the mean pore size, pore volume, and specific surface area can be changed by using a sulfone-containing monomer and the application of this monomer to the gas-separation membrane is expected to help control the permeability and selectivity of the membrane.

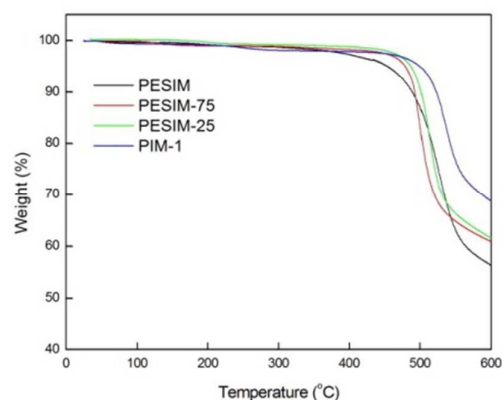


Fig 6. TGA curves of PESIM, PESIM-75, PESIM-25, and PIM-1.

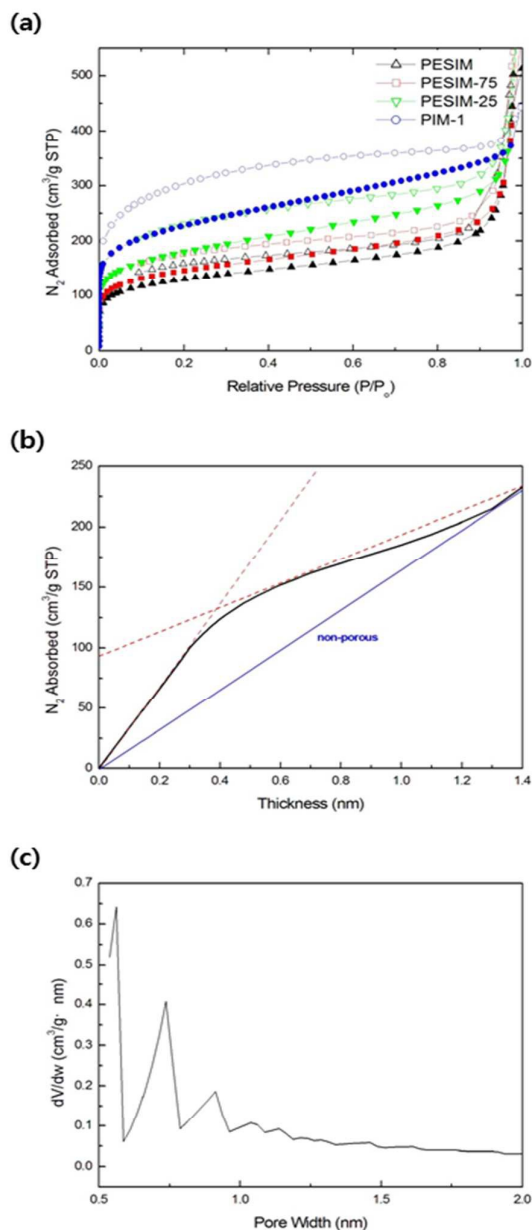


Fig 7. BET analysis of PESIM, PESIM-75, PESIM-25, and PIM-1: (a) Adsorption and desorption isotherms of PESIM, PESIM-75, PESIM-25, and PIM-1 at 77 K, (b) t-plot of PESIM, and (c) H-K plot of PESIM.

Conclusions

In the present study, we synthesized a new type of polyethersulfone with intrinsic micropores and identified its thermal properties and microporosity characteristics. When a monomer with a linear sulfonyl group was introduced to a polymer chain, their thermal properties were maintained. Polyethersulfone polymers and copolymers with intrinsic microporosity showed a high specific surface area of 400–600 m^2g^{-1} . It is believed that characteristic changes in their mean pore size and volume according to copolymerization ratio can

be used as a method for controlling permeability and selectivity when applied to gas-separation membranes.

Acknowledgements

This research was supported by two grants from Industrial Strategic Technology Development Program (the Ministry of Trade, Industry and Energy, Korea, 10052883) and the R&D Convergence Program of NST (National Research Council of Science and Technology, Korea).

Notes and References

- P. M. Budd, E. S. Elabas, B. S. Ghanem, S. Makhseed, N. B. McKeown, K. J. Msayib, C. E. Tattershall, D. Wang, *Adv. Mater.*, 2004, **16**, 456-459.
- P. M. Budd, N. B. McKeown, D. Fritsch, *J. Mater. Chem.*, 2005, **15**, 1977-1986.
- N. B. McKeown, P. M. Budd, K. J. Msayib, B. S. Ghanem, H. J. Kingston, C. E. Tattershall, S. Makhseed, K. J. Reynolds, D. Fritsch, *Chem. Eur. J.*, 2005, **11**, 2610-2620.
- N. du, J. Song, G. P. Robertson, I. Pinnau, M. D. Guiver, *Macromol. Rapid Commun.*, 2008, **29**, 783-788.
- S. Thomas, I. Pinnau, N. du, M. D. Guiver, *J. Membr. Sci.*, 2009, **333**, 125-131.
- J. Song, N. Du, Y. Dai, G. P. Robertson, M. D. Guiver, S. Thomas, I. Pinnau, *Macromolecules*, 2008, **41**, 7411-7417.
- J. Ahn, W. J. Chung, I. Pinnau, J. Song, N. Du, G. P. Robertson, M. D. Guiver, *J. Membr. Sci.*, 2010, **246**, 280-287.
- N. Du, G. P. Robertson, I. Pinnau, S. Thomas, M. D. Guiver, *Macromol. Rapid Commun.*, 2009, **30**, 584-588.
- N. Du, G. P. Robertson, I. Pinnau, M. D. Guiver, *Macromolecules*, 2010, **43**, 8580-8587.
- R. Short, M. Carta, C. G. Bezzu, D. Fritsch, B. M. Kariuki, N. B. McKeown, *Chem. Commun.*, 2011, **47**, 6822-6824.
- N. B. McKeown, P. M. Budd, D. Book, *Macromol. Rapid Commun.*, 2007, **28**, 995-1002.
- N. Du, M. M. Dal-Cin, I. Pinnau, A. Nicalak, G. P. Robertson, M. D. Guiver, *Macromol. Rapid Commun.*, 2011, **32**, 631-636.
- N. Du, G. P. Robertson, J. Song, I. Pinnau, M. D. Guiver, *Macromolecules*, 2009, **42**, 6038-6043.
- B. G. Kim, D. Henkensmeier, H. J. Kim, J. H. Jang, S. W. Nam, T. H. Lim, *Macromol. Res.*, 2014, **22**, 92-98.
- N. Du, G. P. Robertson, I. Pinnau, M. D. Guiver, *Macromolecules*, 2009, **42**, 6023-6030.
- N. Du, H. B. Park, G. P. Robertson, M. M. Dal-Cin, T. Visser, L. Scoles, M. D. Guiver, *Nature Materials*, 2011, **10**, 372-375.
- C. R. Mason, L. Maynard-Atem, K. W. J. Heard, B. Satilmis, P. M. Budd, K. Friess, M. Lanč, P. Bernardo, G. Clarizia, J. C. Jansen, *Macromolecules*, 2014, **47**, 1021-1029.
- C. R. Mason, L. Maynard-Atem, N. M. Al-Harbi, P. M. Budd, P. Bernardo, F. Bazzarelli, G. Clarizia, J. C. Jansen, *Macromolecules*, 2011, **44**, 6471-6479.
- R. Swaidan, B. S. Ghanem, E. Litwiller, I. Pinnau, *J. Membr. Sci.*, 2014, **457**, 95-102.
- E. Madrid, Y. Rong, M. Carta, N. B. McKeown, R. Malpass-Evans, G. A. Attard, T. J. Clarke, S. H. Taylor, Yi-Tao Long, F. Marken, *Angew. Chem.*, 2014, **126**, 10927-10930.
- E. Madrid, P. Cottis, Y. Rong, A. T. Rogers, J. M. Stone, R. Malpass-Evans, M. Carta, N. B. McKeown, F. Marken, *J. Mater. Chem. A*, 2015, **3**, 15849-15853.
- S. Y. Son, Y. J. Noh, C. Bok, S. Lee, B. G. Kim, S. I. Na, H. I. Joh, *Nanoscale*, 2014, **6**, 678-682.

- 23 A. Warshawsky, N. Kahana, A. Deshe, H. E. Gottlieb, R. Arad-Yellin, *J. Polym. Sci.: Part A: polym. Chem.*, 1990, **28**, 2885-2905.
- 24 E. Avram, M. A. Brebu, A. Warshawsky, C. Vasile, *Polym. Degrad. Stabil.*, 2000, **69**, 175-181.
- 25 A. Noshay, L. M. Robeson, *J. Appl. Polym. Sci.*, 1976, **20**, 1885-1903.
- 26 B. Van der Bruggen, *J. Appl. Polym. Sci.*, 2009, **114**, 630-642.
- 27 J. F. Blanco, Q. T. Nguyen, P. Schaetzel, *J. Membr. Sci.*, 2001, **186**, 267-279.
- 28 V. Carlier, J. Devaux, R. Legras, *Macromolecules*, 1992, **25**, 6646-6650.
- 29 J. Wang, Z. Zhao, F. Gong, S. Li, S. Zhang, *Macromolecules*, 2009, **42**, 8711-8717.